CHAPTER 10

Aerothermodynamics of Gas Turbines

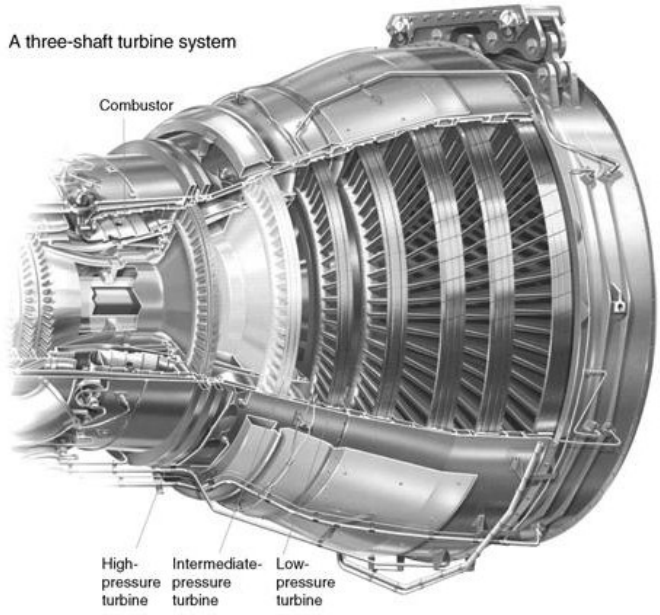

Source: Reproduced with permission from Rolls-Royce plc

10.1 Introduction

Gas turbines produce shaft power for the compressor in the gas generator as well as other external loads, such as the fan in a turbofan, propeller in a turboprop, helicopter rotor in a turboshaft, and electric generator. The high pressure and temperature gas from the combustor enters the gas turbine first through a stationary blade row, known as the nozzle. The first nozzle is thus exposed to the highest gas temperatures in the engine ($T_{t4} \sim$ 1750–2000 K). However, the stationary nature of gas turbine nozzle saves it from an additional centrifugal stress that rotor blades face. Since the gas path temperature is 400–800 K higher than the blade service temperature, all modern gas turbines are cooled. The coolant, which is bled from compressor accounts for ∼10–15% of the airflow rate in the gas generator. A reduction of ∼3% turbine efficiency per 1% cooling flow is attributed to cooling losses. In this chapter, we will introduce aerodynamics of turbine blades, optimal nozzle exit tangential Mach number, optimum solidity, turbine losses, and cooling. We conclude the chapter with axial-flow turbine design and practices and an example. Figure 10.1 shows a schematic drawing of a gas turbine.

10.2 Axial-Flow Turbines

The flowfield in a turbine is dominated by favorable pressure gradients unlike the compressor flow. The boundary layers in a turbine are thus less susceptible to stall than their counterparts in a compressor. The notion that a turbine is a "mirror image" of a compressor

Aircraft Propulsion, Second Edition. Saeed Farokhi.

Companion Website: www.wiley.com/go/farokhi

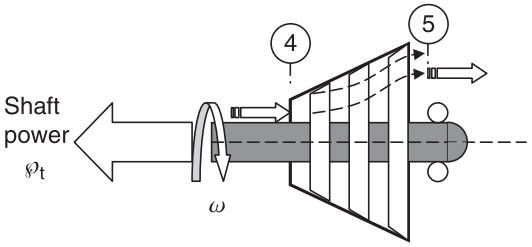

■ **FIGURE 10.1**
Schematic drawing of an axial-flow turbine

is therefore misleading. The evidence of many compressor stages (~5 in modern gas turbine engines of the same mass flow rate) being driven by a single turbine stage is a compelling reason for the inherent differences in the fluid mechanics of the two devices. The challenges in a turbine are primarily in the cooling techniques and their effectiveness; tip clearance control, blade life, and material characteristics suitable for a high-temperature environment and corrosion. In the compressor, the flow stability (rotating stall and surge) and efficiency are highly critical to the design.

The aerodynamics of turbine stages is governed by the conservation principles of mass, momentum, and energy. The conservation of angular momentum is expressed by the Euler turbine equation, which we derived in the early part of Chapter 8. It states that the time-rate-of-change of the fluid angular momentum is balanced by a net external torque that acts on the fluid, namely,

$$\tau_{\text{fluid}} = \dot{m}(r_2 C_{\theta 2} - r_1 C_{\theta 1}) \tag{10.1}$$

Let us show a schematic drawing of a turbine stage, assign station numbers, and show the velocity triangles in the stage. A turbine stage begins with a stationary blade row, known as the nozzle, followed by a rotating blade row, known as the rotor or sometimes bucket. The combustor exit flow is expanded, that is, accelerated, in a turbine nozzle, which converts the fluid thermal energy into the fluid kinetic energy. The inlet flow to the nozzle is typically swirl free and thus the nozzle imparts swirl to the flow. This behavior is opposite to a compressor stator, which removes the swirl from the flow. The nozzle flow is choked over a wide operating range of the engine, and the exit of the nozzle may also operate in the supersonic regime. The rotor blade row follows the nozzle and exchanges energy with the fluid. The rotor thus removes the swirl put in by the nozzle, again an opposite behavior to the compressor rotor. An examination of velocity triangles in a turbine stage (Figure 10.2) reveals the swirl deposition and extraction of the nozzle and the rotor rows in a turbine, respectively.

The sign convention on the swirl velocity component is the same as the compressors, namely, the swirl is considered positive in the direction of the rotor rotation. For example, the inlet swirl upstream of the turbine nozzle is shown in the positive direction in Figure 10.2. The absolute and relative swirls downstream of the nozzle are both in the positive direction, as also shown in Figure 10.2. The relative swirl downstream of the rotor blade has a negative swirl velocity, whereas the absolute swirl is shown in the positive direction.

The power exchange between the rotor and the fluid may be observed in Figure 10.2 as the rotor rotation is in the same direction as the aerodynamic force acting on it in the tangential direction. We may express the rotor shaft power in thermodynamic terms as

$$\wp_{\text{rotor}} = -\wp_{\text{fluid}} = \dot{m}\left(h_{t2} - h_{t3}\right) \tag{10.2}$$

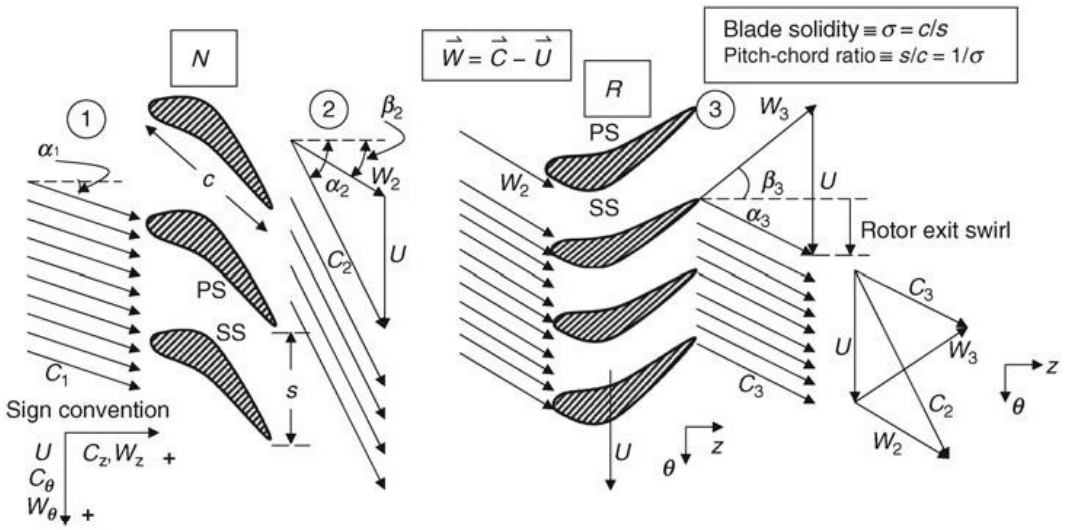

■ **FIGURE 10.2**
Schematic drawing of a turbine stage with velocity triangles, sign convention flow angle definitions, and blade solidity

We may express the rotor power in mechanical terms via the Euler turbine equation as

$$\mathcal{P}_{\text{rotor}} = -\mathcal{P}_{\text{fluid}} = \dot{m}\omega[(r_2 C_{\theta 2}) - (r_3 C_{\theta 3})] \tag{10.3}$$

Since the stator or nozzle puts in swirl, i.e., angular momentum, in the flow and the rotor or bucket removes the angular momentum in a turbine, the bracket on the right-hand side of Equation 10.3 is positive. The implication is that the turbine rotor produces power and the power of the fluid is thus drained or diminished. These are all consistent with our expectations. The turbine nozzle imparts a positive torque on the fluid and thus feels an equal and opposite torque in reaction. We may express the nozzle torque as

$$\tau_{\text{n}} = -\tau_{\text{fluid}} = \dot{m}[(r_1 C_{\theta 1}) - (r_2 C_{\theta 2})] \tag{10.4}$$

From the magnitude of the angular momentum up- and downstream of the nozzle, we note that the fluid torque is positive and the nozzle torque is negative. The rotor toque is

$$\tau_{\text{r}} = -\tau_{\text{fluid}} = \dot{m}[(r_2 C_{\theta 2}) - (r_3 C_{\theta 3})] \tag{10.5}$$

Since the bracket on the right-hand side of Equation 10.5 is positive, as the fluid angular momentum is higher upstream of the rotor than downstream, we may conclude that the torque acting on the fluid is negative and the blade torque is in the positive direction. In case of repeated stages, we have the rotor exit angular momentum equal to the nozzle entrance angular momentum, that is,

$$r_3 C_{\theta 3} = r_1 C_{\theta 1} \tag{10.6}$$

Then the rotor torque becomes equal and opposite the nozzle torque. Consequently, a turbine stage, as a whole, does not impart a net torque on the engine structure.

In axial-flow turbines, as in axial-flow compressors, the radial shift of the stream surfaces is small and usually neglected in a first approximation. A second approximation is made about the constant axial velocity through the stage or the density–velocity ratio

across blade rows in a stage. The choice of the degree of reaction in a turbine ranges from zero to upward of 50%. A zero degree of reaction turbine stage, known as the impulse stage, produces the entire static enthalpy drop of the stage across the nozzle. The rotor produces no static enthalpy drop. The degree of reaction in a turbine is defined as the ratio of static enthalpy drop in the rotor to that of the stage, namely,

$$^{\circ}R \equiv \frac{h_2 - h_3}{h_1 - h_3} \tag{10.7}$$

Let us rewrite Equation 10.7 in terms of the stagnation states and the fluid kinetic energy,

$$^{\circ}R = \frac{h_{t2} - h_{t3} - C_2^2/2 + C_3^2/2}{h_{t1} - h_{t3} - C_1^2/2 + C_3^2/2}$$

Assuming the inlet and exit kinetic energies of the stage are equal, the above expression is simplified to

$$^{\circ}R = 1 - \frac{C_2^2 - C_3^2}{2(h_{t2} - h_{t3})} = 1 - \frac{C_{\theta 2}^2 - C_{\theta 3}^2}{2U(C_{\theta 2} - C_{\theta 3})} = 1 - \frac{C_{\theta 2} + C_{\theta 3}}{2U} = 1 - \frac{C_{\theta \text{mean}}}{U} \tag{10.8}$$

where we have further assumed that the axial velocity remains constant and the radial shift of stream surfaces is small. The form of the degree of reaction, as expressed in Equation 10.8, is identical to the formulation of the compressor degree of reaction. It is the nondimensional average swirl velocity ($C_{\theta \text{mean}}/U$) in the rotor that establishes the degree of reaction at a given radius. Thus, the 50% degree of reaction demands the average swirl in the rotor to be one half of the rotational speed, which suggests a symmetrical velocity triangle across the rotor and nozzle (stator). This behavior is identical to the compressor. The zero degree of reaction, known as the impulse turbine, demands the average swirl in the rotor to be the same as the rotor speed. The velocity triangles and the blade row geometry for an axial exit flow are shown in Figure 10.3.

■ **FIGURE 10.3**
An Impulse and a 50% reaction stage with swirl-free exit flow

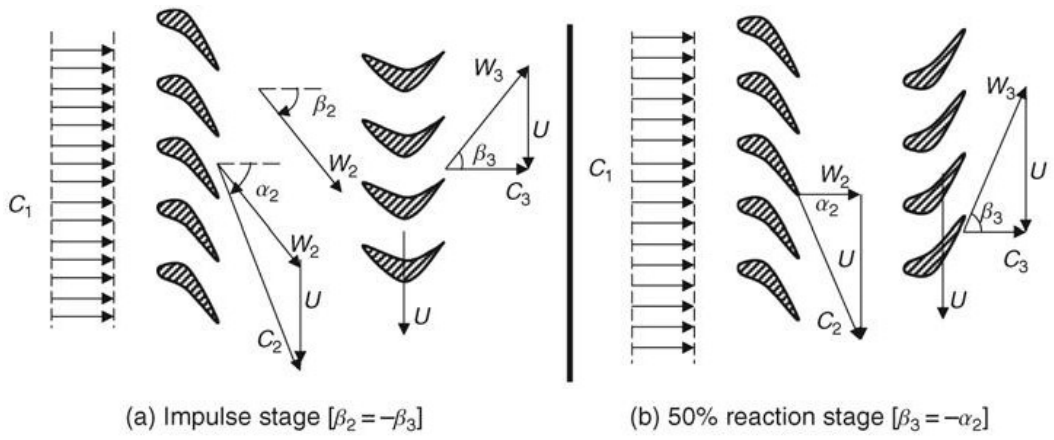

For a 50% degree of reaction turbine stage and a swirl-free exit flow condition, that is, $C_{\theta 3} = 0$, we have

$$C_{\theta \mathrm{m}} = \frac{U}{2} = \frac{C_{\theta 2}}{2} \quad \text{or} \quad C_{\theta 2} = U \tag{10.9}$$

The rotor specific work, via the Euler turbine equation, is

$$w_{\mathrm{t}} \equiv \frac{\mathscr{P}_{\mathrm{t}}}{\dot{m}_{\mathrm{t}}} \cong U\Delta C_{\theta} = U^2 \tag{10.10}$$

or stage loading coefficient ψ is

$$\psi \equiv w_t/U^2 = 1$$

The zero degree of reaction of an impulse turbine stage requires

$$C_{\theta \mathrm{m}} = U = \frac{C_{\theta 2}}{2} \quad \text{or} \quad C_{\theta 2} = 2U \tag{10.11}$$

The rotor specific work for an impulse turbine is, therefore,

$$w_{\mathrm{t}} \equiv \frac{\mathscr{P}_{\mathrm{t}}}{\dot{m}_{\mathrm{t}}} \cong U\Delta C_{\theta} = 2U^2 \tag{10.12}$$

or stage loading coefficient ψ is

$$\psi \equiv w_t/U^2 = 2$$

Comparing the specific work of the rotors from Equations 10.10 and 10.12, we note that the impulse design produces twice as much shaft power per unit mass flow rate than the 50% reaction turbine for the same rotor speed U. Although the impulse turbine designs have the potential of producing large specific works, they are less efficient than the reaction type turbines. The primary reason is in the rotor where the relative flow speed remains constant and, hence, the viscous flow losses are larger than reaction turbines where the flow continuously accelerates. It is also instructive to show the thermodynamic states of the gas in both types of turbine stages on a T–s diagram. Figure 10.4 shows the static and total (or stagnation) states of the fluid in a reaction turbine stage, that is, $^{\circ}R > 0$.

We note that the static temperature drop occurred across the nozzle as well as the rotor. Therefore, the turbine stage that is shown in Figure 10.4 is a reaction turbine.

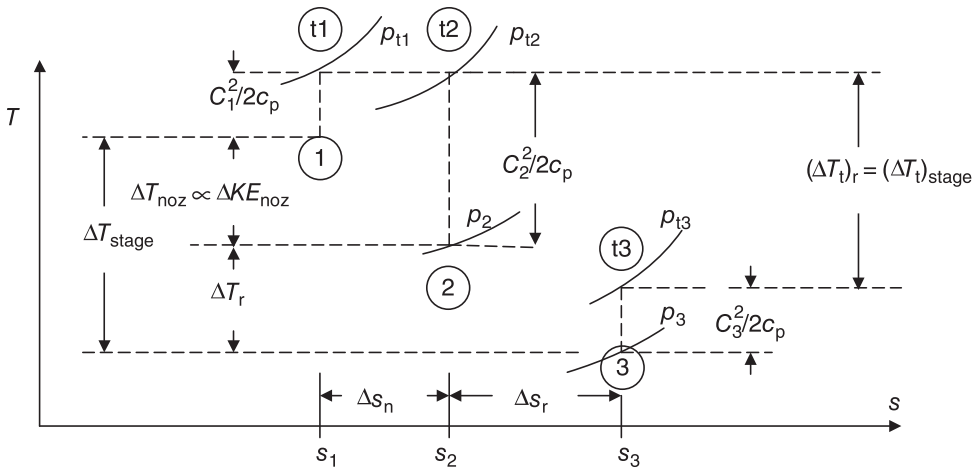

■ **FIGURE 10.4** ***T–s*** **diagram of thermodynamic states of gas in a reaction turbine stage**

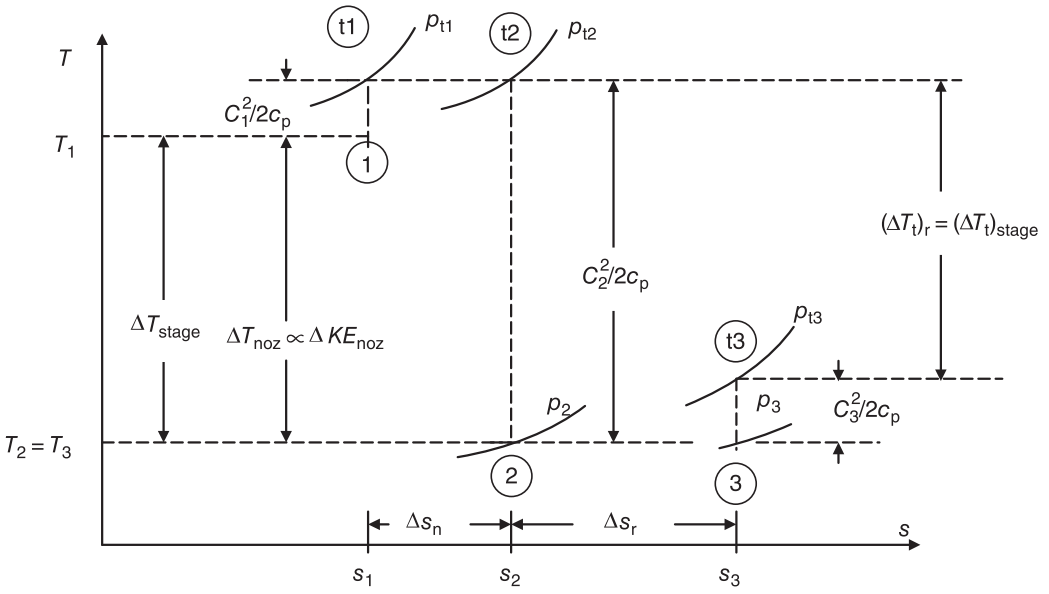

■ **FIGURE 10.5**
Thermodynamic states of gas in an impulse turbine stage ($^\circ R = 0$) show a large power production capability, $\propto (\Delta T_t)_{stage}$

The stage work may also be noted in Figure 10.4 as proportional to the stage total temperature drop. The nozzle suffers some total pressure loss $p_{t1} - p_{t2}$ due to viscous effects in the boundary layer and possible shock losses. The rotor loss may be observed in the entropy rise Δs_r in Figure 10.4. The thermodynamic states of gas in an impulse turbine stage, for comparison purposes, are shown in Figure 10.5.

Similar observations to the reaction turbine may also be made on the impulse stage, as shown in Figure 10.5. One exception is that the static temperature change across the rotor is zero in the impulse turbine. Consequently, the static temperature drop ΔT_{stage} occurs solely across the nozzle. Also, we note a large expansion across the nozzle, as evidenced by a large ΔT_{noz}, as compared with the reaction type turbine. The entropy rise in an impulse stage is intentionally depicted as larger than the corresponding entropy rise in the reaction turbine stage to signify higher losses. We also note that the rotor specific work, which is proportional to the total temperature drop across the rotor, is depicted roughly twice as much (in Figure 10.5) as the reaction turbine stage of Figure 10.5 to reflect Equations 10.10 and 10.12. In some texts (e.g., Dixon, 1975), an impulse stage is defined as having zero static pressure drop across the rotor. In this case, then a zero-reaction turbine, which has its static enthalpy constant across the rotor, is not strictly speaking an impulse stage. In a zero-reaction turbine, there is still some static pressure drop due to frictional losses within the blade. Thus, an impulse turbine would have a slightly negative degree of reaction. In this book, the words impulse and zero reaction are interchangeably used, albeit more loosely than the strict classical definition.

The turbine specific work could be expressed in terms of the nozzle exit flow angle α_2 and the condition of zero swirl at the rotor exit as

$$w_t = U(C_{\theta 2} - C_{\theta 3}) \approx UC_{\theta 2} = UC_{z2} \tan \alpha_2 \qquad \textbf{(10.13)}$$

For a constant axial flow velocity C_z, we note that the rotor work per unit mass flow rate increases linearly with the increase in wheel speed U and (nonlinearly with) the flow turning angle α_2 through the tangent of α_2 term in Equation 10.13. For practical reasons,

the flow angle at the nozzle exit is limited to $\sim 70°$, otherwise flow losses become excessive, that is,

$$\boxed{\alpha_{2,\max} \approx 70°} \tag{10.14}$$

The wheel speed U is a quadratic contributor to the blade centrifugal stresses σ_c; hence, it is limited by the structural stresses and the blade life requirements. To gain further insight, we may cast the above equation in terms of the blade tangential and the flow Mach numbers downstream of the nozzle as

$$w_t = UC_2 \sin\alpha_2 = a_2^2 M_T M_2 \cdot \sin\alpha_2 = a_{t2}^2 \cdot M_T M_2 \sin\alpha_2 \Big/ \left[1 + \left(\frac{\gamma - 1}{2}\right) M_2^2\right] \tag{10.15}$$

Since the stagnation temperature does not change across the nozzle, the stagnation speed of sound at 2 is the same as 1, hence proportional to the combustor exit total temperature T_{t4}, a cycle parameter. We may conclude from Equation 10.15 that to maximize the rotor specific work, we need to have high inlet stagnation temperatures, T_{t1} (or T_{t4} from our cycle analysis notation), a high tangential Mach number of the blade, M_T, a high swirl Mach number at the nozzle exit, $M_2 \sin\alpha_2$. The blade tangential Mach number M_T has a maximum at the rotor blade tip radius M_T (r_t). The high gas temperatures in the high-pressure turbine (HPT) demand internal cooling of the rotor blades. A cooled rotor blade leading edge needs to be blunt to allow for sufficient surface area to cool, as it represents the stagnation point of the blade with the attendant high heat flux. A blunt leading edge is best suited for a subsonic relative flow, which then limits the maximum M_T parameter in the HPT. In the low-pressure turbine (LPT), the gas temperature is significantly reduced, hence internal cooling of the blades may not be required at all. Therefore, the rotor tip in the LPT may operate with a sharp leading edge, which is then suitable for a supersonic operation. In addition, the speed of sound for the first rotor is about $\sim \sqrt{1/\tau_t}$ higher than the speed of sound in the last rotor. This means that for the same tip speeds, ωr_t, the blade tangential Mach number is higher in the LPT than the HPT, that is, inversely proportional to the local speed of sound. These arguments are made to show the conflicting requirements of internal cooling (due to high gas temperatures) and centrifugal stresses with the desire to operate the turbine rotors with a supersonic tip to maximize the rotor work output. Let us summarize the parameter trends in reaction and impulse turbine stages graphically in Figures 10.6 and 10.7, respectively.

We have examined parameter trends in turbine stages with *zero exit swirl* in Figures 10.6 and 10.7. Let us provide a rationale for that. The swirl in the exit flow does not contribute to the thrust production, which is the function of our engine, and even increases the total pressure loss in the nozzle. Consequently, it is desirable to design a turbine stage with zero exit swirl. Also, we have depicted the streamtubes upstream and downstream of the turbine blades with corresponding flow areas A_1 and A_2 for the nozzle and A_{2r} and A_{3r} in the rotor frame of reference for the rotor. In a reaction turbine, the streamtube flow areas continually shrink, as flow continually accelerates in the blade rows. In the impulse stage, the relative flow in the rotor attains a constant speed and thus the relative streamtube does not shrink. Thus, the static temperature remains constant and the static pressure remains unchanged in the limit of inviscid flow and drops with frictional losses in the boundary layers. The relative flow downstream of the rotor in an impulse stage is the mirror image of the relative flow upstream of the rotor (Figure 10.7). Also note that the choice of constant

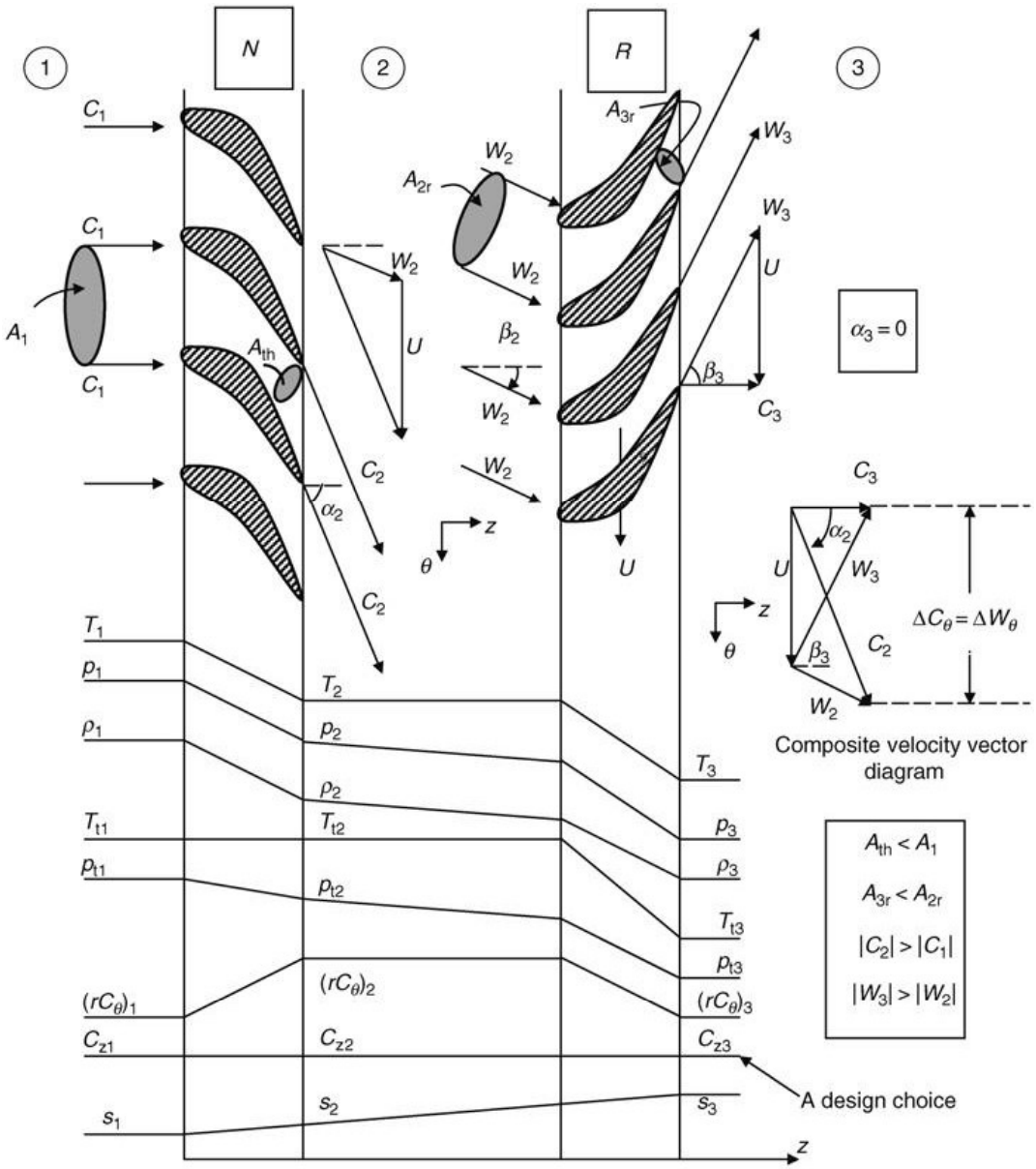

■ **FIGURE 10.6**
Parameter trends in a reaction turbine stage with zero exit swirl and designed for constant axial velocity (in an uncooled stage)

axial velocity C_z, as shown in Figures 10.6 and 10.7, is depicted as a design choice, similar to a compressor. The annulus sizing and the geometry are directly affected by our choice of the axial velocity and the mass flow rate through continuity equation. With a constant axial velocity and a decrease in gas density in the flow direction, the annulus flow area needs to grow inversely proportional to the density drop. In the case of a cooled turbine, the coolant mass flow rate needs to be added to the hot gas flow rate in establishing the annulus flow area, via continuity equation. Now, let us examine the design parameters that affect the mass flow rate in a turbine stage, the power production, and the turbine efficiency. Three turbine annuli are shown in Figure 10.8 and the station numbers at the entrance and exit correspond to our cycle analysis notation, stations 4 and 5, respectively. In this example, we show three types of annuli: the first has a constant tip radius, i.e., the casing is of cylindrical shape, and a variable hub radius for the annulus geometry (Figure 10.8a);

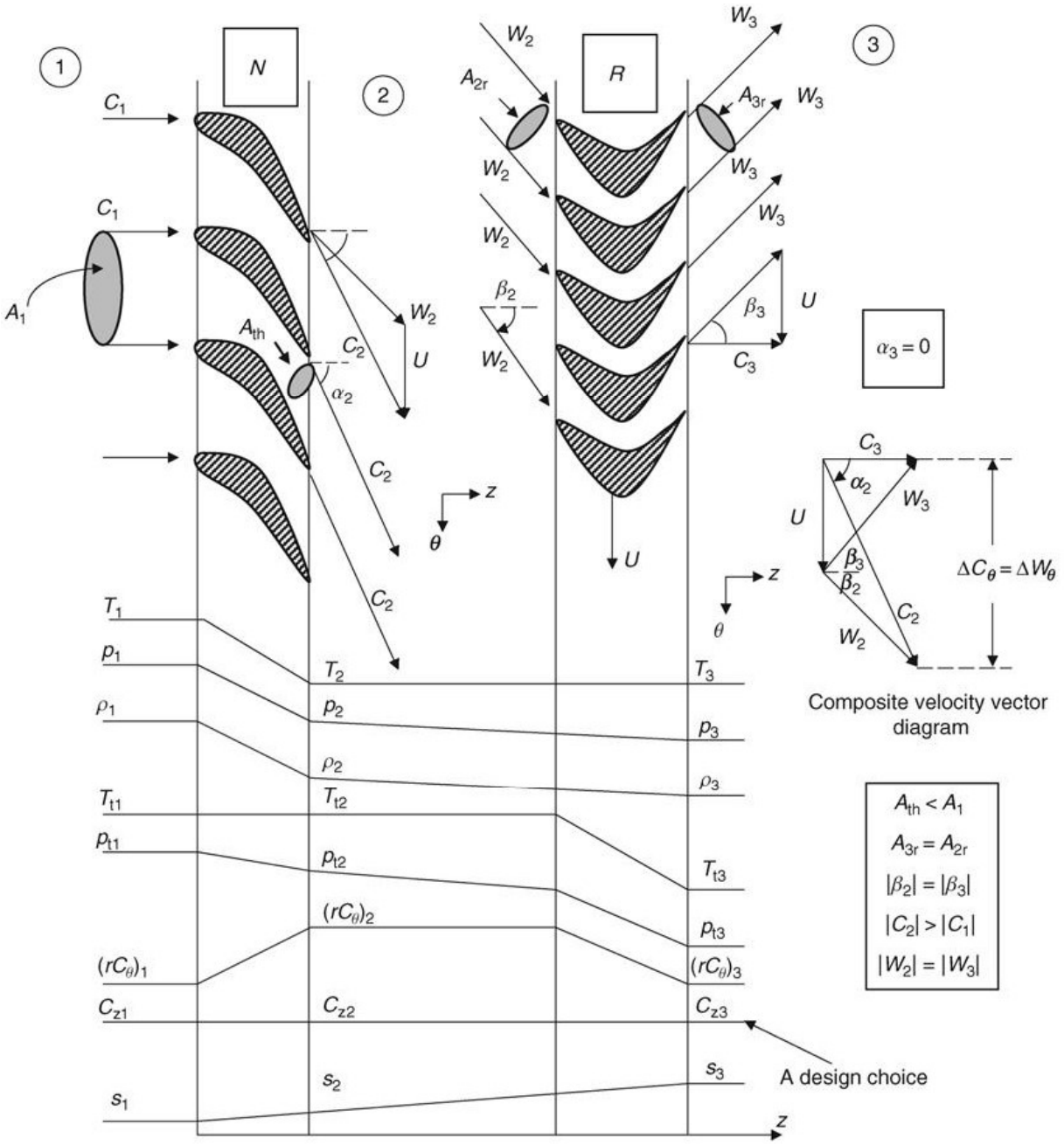

■ **FIGURE 10.7** **Parameter trends in an impulse turbine stage with zero exit swirl and designed for constant axial velocity (in an uncooled stage)**

the second has constant hub radius (Figure 10.8b); and the third has a varying hub and casing radii (Figure 10.8c). In a mixed-stream turbofan engine, the choice of constant tip radius for the outer casing of the turbine annulus leads to a better integration of the cold and hot streams in a forced mixer. The second advantage of a constant outer radius is in lower centrifugal stresses of the rotor blades, simply by the virtue of a smaller moment arm. The third advantage is in engine frontal area and weight. Integration with the turbine aft-cone in aircraft gas turbine engines will also benefit from a tapered hub radius, as shown schematically in Figure 10.8a. In some applications, for example, stationary gas

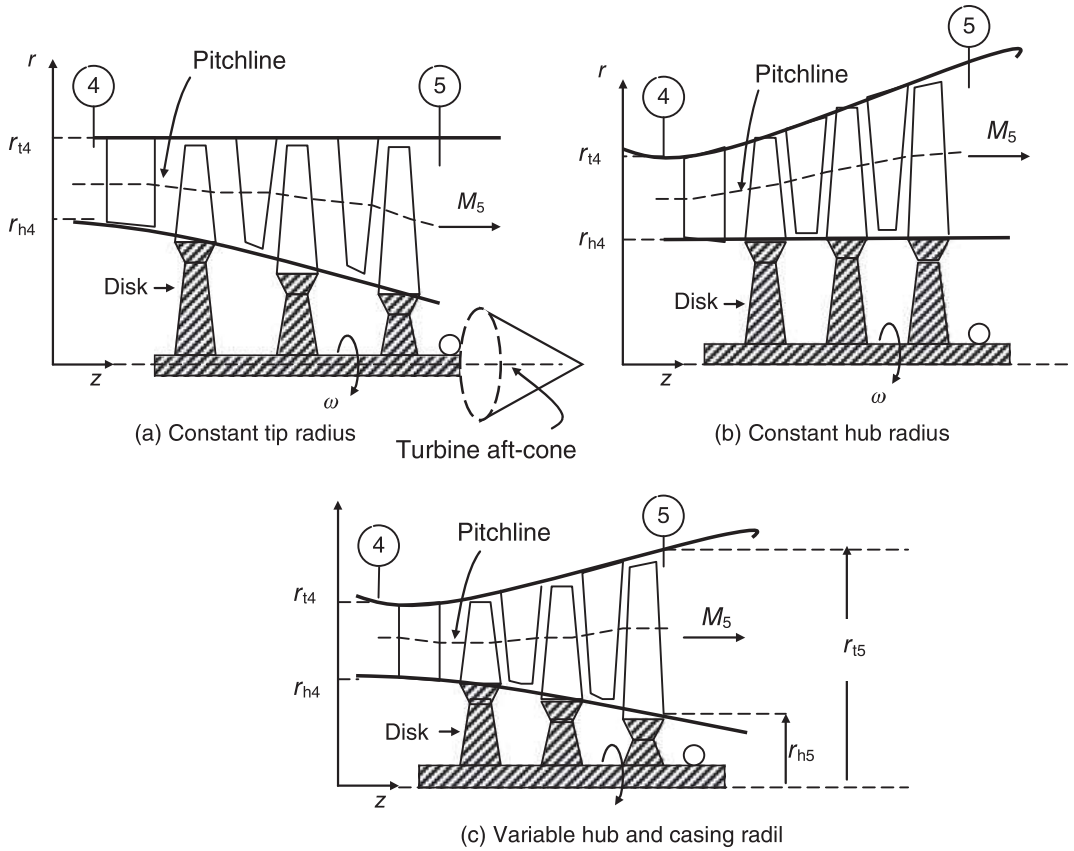

■ **FIGURE 10.8**
Schematic drawing of the geometry of three turbine annuli

turbine power plants, the choice of constant hub radius is considered advantageous, as it integrates with an annular exhaust diffuser as well as reduces manufacturing costs of the turbine rotor disks (i.e., all with the same diameter). The varying hub and tip case shown schematically in Figure 10.8c offers a constant radius pitchline advantage, but at an increased manufacturing costs and, potentially, an increased weight over the first two designs. In general, a turbine annulus with an increasing tip radius adds weight to the rotor disks and turbine overall weight.

Our one-dimensional continuity equation written between stations 4 and 5 yields

$$\dot{m}_4 = \sqrt{\frac{\gamma_4}{R_4}}\frac{p_{t4}}{\sqrt{T_{t4}}}A_4 M_4\left(1+\left(\frac{\gamma_4-1}{2}\right)M_4^2\right)^{-\frac{\gamma_4+1}{2(\gamma_4-1)}} = \dot{m}_5$$
$$= \sqrt{\frac{\gamma_5}{R_5}}\frac{p_{t5}}{\sqrt{T_{t5}}}A_5 M_5\left(1+\left(\frac{\gamma_5-1}{2}\right)M_5^2\right)^{-\frac{\gamma_5+1}{2(\gamma_5-1)}} \tag{10.16}$$

Since the exit of the nozzle remains choked over a wide operating range of the engine, it is more convenient to use $M_4 = 1$ and $A4$ as the choked throat area of the turbine nozzle. Therefore, the annulus area ratio A_5/A_4 becomes

$$\frac{A_5}{A_4} = \sqrt{\frac{\gamma_4/\gamma_5}{R_4/R_5}}\frac{1}{M_5}\frac{\sqrt{\tau_t}}{\pi_t}\frac{\left(1+\left(\frac{\gamma_5-1}{2}\right)M_5^2\right)^{\frac{\gamma_5+1}{2(\gamma_5-1)}}}{\left(2/(\gamma_4+1)\right)^{\frac{\gamma_4+1}{2(\gamma_4-1)}}} \tag{10.17}$$